COMSOL CONFERENCE 2023 MUNICH

Finite Element Analysis of Friction Stir Welding of Al Alloy and Inconel 718

A. Abotaleb[1*], Y. Remond[1], M. Khraisheh[2], S. Ahzi[1]
[1]University of Strasbourg, ICUBE laboratory – CNRS, 2 Rue Boussingault, 67000 Strasbourg
[2]Mechanical Engineering Program, Texas A&M University at Qatar, Doha, Qatar
*Corresponding Author: ahmed.abotaleb@etu.unistra.fr

Abstract
Friction Stir Welding (FSW) is a solid-state joining technique that has become increasingly popular and efficient for welding both similar and dissimilar metallic materials. Despite its success in joining dissimilar materials, further development is necessary to meet industry requirements and improve understanding of the FSW process. The welding of nickel-based superalloys such as Inconel 718 presents technical challenges, with limited literature suggesting that the process is only achievable at high axial forces and selective process parameters, limiting its industrial applications. To address these challenges, this study proposes 3D finite element models that couple multiphysics, including material flow and heat transfer via conduction, convection, and radiation. A 3D thermo-mechanical model was developed in COMSOL Multiphysics v 5.3 to simulate the FSW process. The model was validated against published experimental results for Al alloys and extended to Inconel 718. The models were used to investigate the temperature and strain distribution in the nugget region, thermo-mechanically affected region, and heat-affected region. The highest temperature recorded for the Al plates was 676°C at the welding joint, exhibiting a heat dissipation pattern across the aluminum plates ranging from 200 to 600°C. These results emphasize the complexity of heat transfer during the FSW process and the significance of considering temperature distribution for successful welding outcomes. In contrast, the 3D temperature profile of the Inconel plates indicated a peak temperature of approximately 1300°C, localized exclusively to the welding regions. Further insight was obtained from the 2D cross section, revealing a maximum temperature concentration around the welding regions and a relatively uniform distribution in the x-direction. These findings highlight the more focused temperature distribution of Inconel 718 around the welding regions, implying enhanced heat dissipation across the plates. Consequently, Inconel 718 may possess improved resistance to thermal degradation and an extended lifespan in high-temperature applications. This information can be used to optimize the FSW process and improve the quality of the resulting welds.

Keywords: Friction stir welding; Finite element analysis; multiphysics modelling; Aluminum alloy; Inconel 718

1. Introduction

Friction is a powerful heat source that can be used to process metals and alloys by welding and depositing. Over the past two decades, there have been significant advancements in friction-based technologies. These techniques rely on friction generated at the surface to form a weld or deposit. Friction stir techniques also use the layer-by-layer building principle of additive manufacturing. They offer several advantages over fusion-based techniques, such as low porosity, reduced distortions, and improved metallic properties. Other potential benefits of friction stir techniques include fine-grained microstructures, high-strength components, and no limitations on build volume. This is largely due to the intense plastic deformation that occurs during the process. Friction stir techniques can be classified into three categories: welding, processing, and advanced processes[1-5].

The evolution of advanced manufacturing depends on new innovative and cutting-edge research activities associated with the fabrication processes, materials, and product design. As most of the advanced manufacturing processes utilize heating and/or generate heat during the production of parts, the modeling of heat transfer related phenomena is of crucial importance, because it directly affects the dimensional accuracy of the parts, their microstructure (porosity, anisotropy, …), their mechanical properties, and their surface quality[6, 7]. In this study we will address one of the main manufacturing processes named friction stir welding (FSW). It is a solid-state welding process that utilizes a non-consumable tool to weld workpieces without reaching the material's melting temperature[8, 9]. It is worth mentioning that, FSW technology was invented twenty years ago in UK at The Welding Institute (TWI).

To accurately predict the quality of a FSW process, it's important to have a deep understanding of the variables that influence it. However, collecting all the necessary information during the FSW process can be difficult due to its complexity[10, 11]. To address this issue, finite element (FE) modeling can be used as an efficient tool to reduce the need for initial experimental trials and help achieve optimized welding parameters[12, 13]. FE simulation of FSW, which involves plastic deformation, heat flow, material flow, and friction, is a challenging task that requires consideration of the nonlinear and thermomechanical processes involved[14]. In recent years, different modeling approaches such as computational fluid dynamics (CFD), Arbitrary Lagrangian-Eulerian (ALE), and Coupled Eulerian-Lagrangian (CEL) have made progress in simulating FSW processes.

The first approach to modeling FSW is using CFD, which treats the workpieces as a non-Newtonian fluid and analyzes the thermo-mechanical behavior

using equations for energy, momentum, and mass conservation[15]. Seidel and Reynolds developed a 2D thermal model based on fluid mechanics that looked at material flow in FSW joints. Their model considered the FSW process as a steady-state, laminar flow of a non-Newtonian fluid past a rotating circular cylinder representing the FSW tool pin. The results showed that the material flow was not symmetrical about the welding centerline and that there was significant vertical mixing during FSW. However, the authors noted a discrepancy between their model and experimental results due to the absence of the tool shoulder, which plays an important role in the mixing process.

The goal of this work is to use numerical methods to study the friction stir welding process of Inconel 718 with the aim of producing high-quality welds under optimized process parameters, such as high tool rotations, fast welding speeds, and lower axial loads. The model will first be tested on aluminum alloys, which are a commonly used material and have been well studied in the literature, to validate its accuracy. After being verified, the model will then be applied to Inconel 718 to evaluate its welding performance, with a focus on the temperature distribution and strain rates.

2. Numerical Model / Methods

The effect of process parameters on temperature, material flow, and strain rate during friction stir welding of Al alloys and Inconel 718 was investigated through numerical modeling using a 3D thermo-mechanical model developed in COMSOL Multiphysics v 5.3. The model was validated against published experimental results for Al alloys before being extended to Inconel 718. The model geometry was built as two plates to accommodate future work of dissimilar materials welding. The plate dimensions are 400-by-102-by-12.7 mm, surrounded by two infinite domains in the x direction. Figure 1 reflects the system geometry.

In this study, a different approach was taken to model the tool in friction stir welding simulations. Instead of treating the tool as a moving heat source, a moving coordinate system was used, which was fixed to the tool axis. This approach involved the use of two infinite element domains, one before and one after the welding zone, to model an infinitely long plate. The rotating tool was then divided into two parts: a pin with an inner contact and a shoulder with a contact surface on the plate. It should be noted that the shoulder was not included in the representation of the model (See Figure 1). Moreover, the heat fluxes generated by friction between the rotating tool and the contact surfaces are considered in the model and are proportional to the normal force and rotating speed. If the temperature exceeds the melting temperature, the heat fluxes from friction are set to zero. The plate also experiences heat transfer by surface-to-ambient radiation and convection. The right side of the infinite plate, which corresponds to the supply side, is assumed to be at ambient temperature.

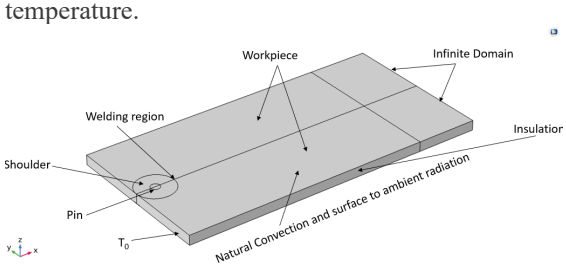

Figure 1. Model Geometry and system domain

The accuracy of simulations for FSW relies heavily on correctly defining the properties of the base material. During FSW, the temperature ranges from room temperature to just below the solidus temperature, and metal properties change with temperature. To ensure accuracy, the relevant mechanical and physical properties of the base materials (Al-T6 and Inconel 718) were defined as temperature-dependent. In addition to temperature changes, the base metal is also subjected to complex strains and strain rates during the welding process. To model the plastic behavior of the base metal, the Johnson-Cook constitutive model was used. This is an empirical viscoplastic model that depicts the work hardening, thermal softening, and strain rate hardening of the metal, making it suitable for high strain-rate deformation and temperature. The von Mises flow stress (σ_o) can be calculated using this model. In addition, average grain size has been estimated based on Zener–Hollomon parameter, which will be further used to estimate the hardness through Hall–Petch relationship.

2.1 Governing Equations

Equation 1 describes the heat transfer in the plate including both the convection and conduction effect.

$$\rho C_p \mathbf{u} \cdot \nabla T + \nabla \cdot (-k \nabla T) = Q \tag{1}$$

The surface heat source represents the heat generated between the workpieces and the tool's pin.

$$q_{\mathrm{pin}}(T) = \frac{\mu}{\sqrt{3(1+\mu^2)}} r_{\mathrm{p}} \omega \bar{Y}(T) \tag{2}$$

The heat generated from the friction of the workpieces and the tool's shoulder is represented in Equation.3, where it is counted as heat flux (W/m^2) at r distance from the center axis.

$$q_{\mathrm{shoulder}}(r,T) = \begin{cases} (\mu F_{\mathrm{n}}/A_{\mathrm{s}})\omega r & \text{if } T < T_{\mathrm{melt}} \\ 0 & \text{if } T \geq T_{\mathrm{melt}} \end{cases} \tag{3}$$

When the local temperature record value equal or higher than the plate melting point, the friction between the tool and the plate can be neglected and accordingly there is not any heat generation. Finally, the heat loss due to the natural convection and surface-ambient radiation to and from the surroundings are considered in Equation 4.

$$q_{\mathrm{u}} = h_{\mathrm{u}}(T_0 - T) + \varepsilon\sigma(T_{\mathrm{amb}}^4 - T^4) \tag{4}$$

$$q_{\mathrm{d}} = h_{\mathrm{d}}(T_0 - T) + \varepsilon\sigma(T_{\mathrm{amb}}^4 - T^4)$$

Johnson-Cook model for flow stress behavior (5)

$$\sigma_{JC} = [A + B\varepsilon^{n}]\cdot\left[1 + C\ln\left(\frac{\dot{\varepsilon}}{\dot{\varepsilon}_0}\right)\right]\cdot\left[1-\left(\frac{T - T_0}{T_m - T_0}\right)^{m}\right]$$

Zener–Hollomon parameter for microstructure change (6)

$$Z = \dot{\epsilon}_e \exp\left(\frac{Q}{RT}\right)$$

Average grain size (7)

$$\ln(d) = 9 - 0.27\ln(Z)$$

Hall–Petch relationship for microhardness estimation (8)

$$H_v = 40 + 72d^{-1/2}$$

Thermal Softening for Inconel 718, modified JC model (9)

- $T < 700$ °C $T_0 = 21$ m=2
- $T \geq 700$°C
  T_0=700 m=0.0016*T+2.0031

2.2 Model Assumptions and Boundary Conditions

- Welding process under ambient conditions without any external heating/cryogenic cooling.
- The shoulder moves in the X-direction without inclination.
- Workpiece and pin physical properties (Thermal conductivity, heat capacity, density, etc.) are function of temperature.
- ε=0.3, μ = 0.4
- h_u = 12.25 W/(m^2·K) and h_d = 6.25 W/(m^2·K).
- The system boundary conditions are reflected in Table 1.
- Time dependent study.

Table 1. Process Parameters for Aluminum alloy and Inconel 718.

Parameter	Unit	Al-T6	Inconel 718
Workpiece melting temperature	°C	660	1260 - 1336
Welding speed	mm/s	1.59	1.65
Rotation Speed	RPM	637	400
Normal Force	kN	25	12.6
Activation energy of lattics diffusion	kJ/mol	140	320
Initial yield stress, sigmags	MPa	324	1350
Strength coefficient, k_jcook	MPa	114	1139
Hardening exponent, n_jcook	-	0.42	0.6522
Strain rate strength coefficient, C_jcook	-	0.002	0.0134
Reference strain rate, $\boldsymbol{\varepsilon}$_jcook	S^{-1}	1	1
Temperature exponent, m_jcook	-	1.34	Fn(T), Eqn (9)

2.3 Meshing system

In this study (see Figure 2), a mesh of 92,000 elements made up of a mix of tetrahedral, prisms, triangles, and quads was used, resulting in an average element quality of 0.786.

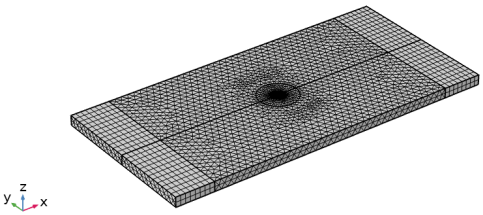

Figure 2. System mesh

3. Simulation Results / Discussion

The finite element model has been validated against published experimental results[16] on aluminum plates, where the plate temperature at 5 mm from the welding nugget zone recorded experimentally at 577°C, while it shows 600°C from the developed COMSOL Multiphysics model reported in this work which reveal a 4% error.

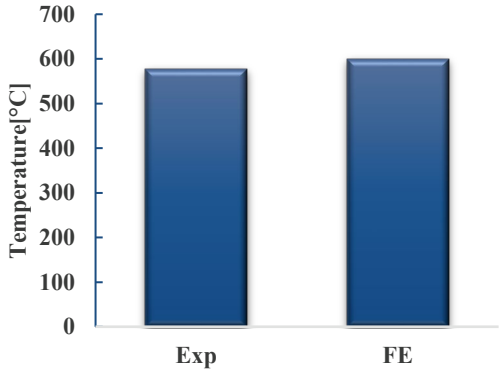

Figure 3. Model validation aluminum plates, 5 mm from the welding nugget zone.

The 3D temperature profile of the aluminum plates displayed in Figure 4 highlights the distribution of heat during the welding process. As observed from the figure, the highest temperature was recorded close to the welding joint with a value of 676 °C. The 2D cross-sectional view of the temperature profile also reveals a heat dissipation pattern across the aluminum plates, ranging from 200 to 600 °C. These results demonstrate the complexity of heat transfer during the FSW process and the importance of considering the temperature distribution for a successful welding outcome. The information obtained from the temperature profile can be used to

optimize the welding process and improve the quality of the resulting welds.

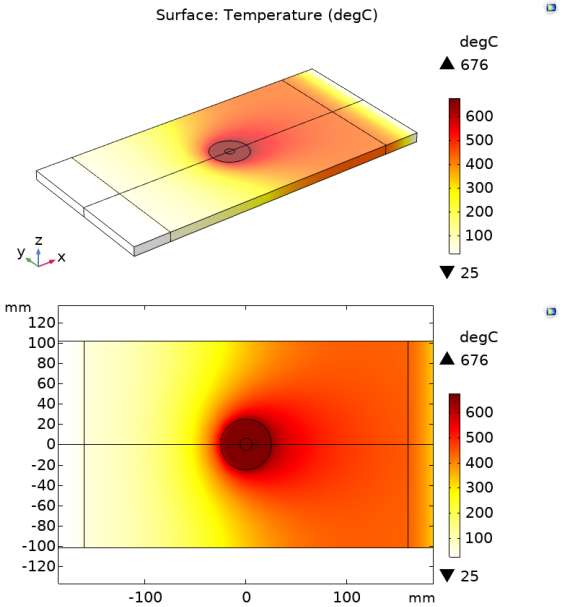

Figure 4. 3D and 2D temperature profile for Al workpiece.

The 1D temperature profile for the aluminum workpiece across the plate length is shown in Figure 5, where the temperature peaked at around 350°C, 20 mm from the welding centerline. It stabilizes just a few seconds after welding. Meanwhile, the temperature profile across the plate thickness is reflected in Figure 6, displaying an almost isothermal profile, ensuring thorough mixing between the plates. On the other hand, the average grain size is depicted in Figure 7, showing grain sizes of around 700µm. Furthermore, microhardness was calculated and is presented in Figure 8, revealing differences in hardness at the welding nugget, thermomechanically affected zone, and heat-affected zone. The microhardness of the aluminum workpiece is around at 43 at the welding nugget zone.

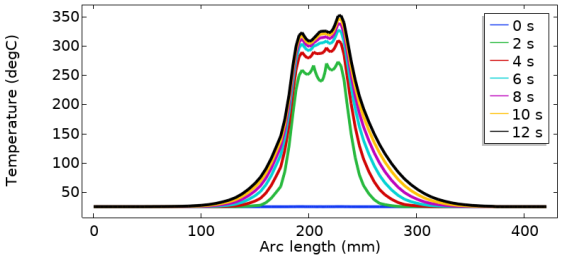

Figure 5. 1D Temperature profile for Al workpiece across welding centerline

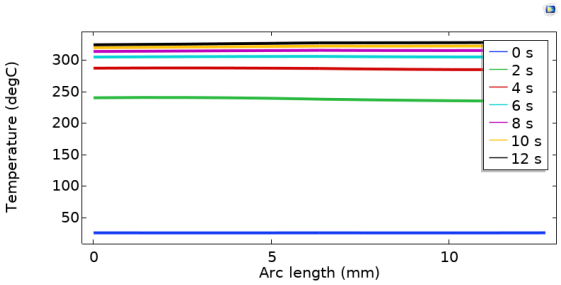

Figure 6. 1D Temperature profile for Al workpiece across plate thickness

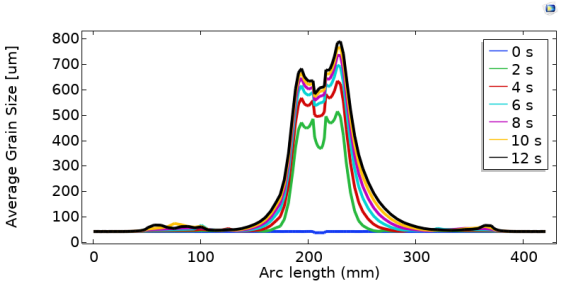

Figure 7. Average grain size for Al workpiece

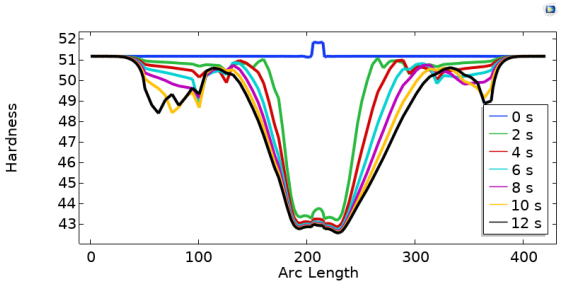

Figure 8. Microhardness for Al workpiece

On the other hand, the results of the 3D temperature profile of the Inconel plates are presented in Figure 9. The findings indicated that the peak temperature was recorded around 1300°C, which was localized to the welding regions only. The 2D cross section provides further insight into the temperature distribution across the plates, where the maximum temperature was focused around the welding regions with an almost uniform distribution in the x-direction. These results demonstrate that the temperature distribution of the Inconel 718 is more focused around the welding regions, resulting in better heat dissipation across the plates. This suggests that Inconel 718 may have better resistance to thermal degradation and a longer lifespan in high temperature applications.

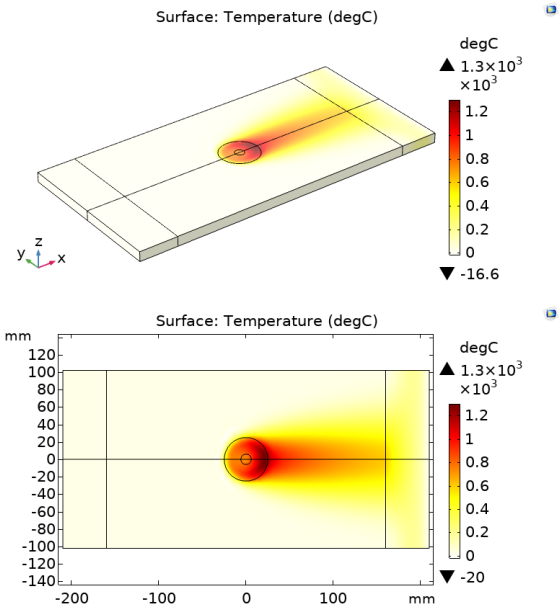

Figure 9. 3D and 2D temperature profile for Inconel 718 workpiece.

Finally, the temperature profile across the plate thickness is reflected in Figure 10, displaying temperature gradient of 120°C, ensuring high heat dissipation between the plates.

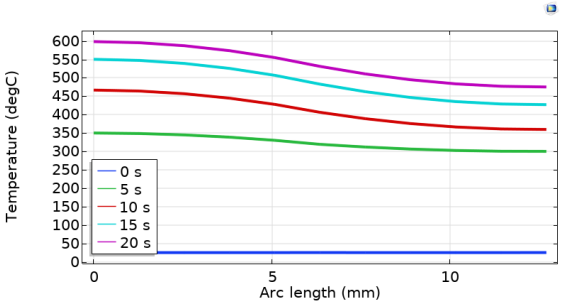

Figure 10. 1D Temperature profile for Inconel-718 workpiece across plate thickness

4. Conclusions

This study focused on the numerical modeling of friction stir welding of Al alloy and Inconel 718 using the COMSOL Multiphysics software. The results of this study provide a better understanding of the effect of process parameters on temperature, material flow and strain rate. A 3D transient non-isothermal CFD model was built to better understand the effect of process parameters on temperature and eventually on material flow and strain rate. It is of particular interest to account for material softening phenomena at elevated temperatures and extremely high strain rates that occur during the FSW process. The fully coupled thermo-mechanical model was validated against experimental results for Al workpieces. The study also found that the developed model could be used to accurately estimate the temperature profile, average grain size, and microhardness of the material.

References

1. Yu, H.Z. and R.S. Mishra, *Additive friction stir deposition: a deformation processing route to metal additive manufacturing.* Materials Research Letters, 2021. **9**(2): p. 71-83.
2. Haghshenas, M. and A.P. Gerlich, *Joining of automotive sheet materials by friction-based welding methods: A review.* Engineering Science and Technology, an International Journal, 2018. **21**(1): p. 130-148.
3. Srivastava, M., et al., *A Review on Recent Progress in Solid State Friction Based Metal Additive Manufacturing: Friction Stir Additive Techniques.* Critical Reviews in Solid State and Materials Sciences, 2019. **44**(5): p. 345-377.
4. Khodabakhshi, F. and A.P. Gerlich, *Potentials and strategies of solid-state additive friction-stir manufacturing technology: A critical review.* Journal of Manufacturing Processes, 2018. **36**: p. 77-92.
5. Palanivel, S. and R.S. Mishra, *Building without melting: a short review of friction-based additive manufacturing techniques.* International Journal of Additive and Subtractive Materials Manufacturing, 2017. **1**(1): p. 82-103.
6. Yunus, M. and M.S. Alsoufi, *Mathematical Modelling of a Friction Stir Welding Process to Predict the Joint Strength of Two Dissimilar Aluminium Alloys Using Experimental Data and Genetic Programming.* Modelling and Simulation in Engineering, 2018. **2018**: p. 4183816.
7. Pan, W., et al., *A new smoothed particle hydrodynamics non-Newtonian model for friction stir welding: Process modeling and simulation of microstructure evolution in a magnesium alloy.* International Journal of Plasticity, 2013. **48**: p. 189-204.
8. Franke, D., et al., *Understanding process force transients with application towards defect detection during friction stir welding of aluminum alloys.* Journal of Manufacturing Processes, 2020. **54**: p. 251-261.
9. Mishra, R.S., et al., *High strain rate superplasticity in a friction stir processed 7075 Al alloy.* Scripta Materialia, 1999. **42**(2): p. 163-168.
10. Assidi, M., et al., *Friction model for friction stir welding process simulation: Calibrations from welding experiments.* International Journal of Machine Tools and Manufacture, 2010. **50**(2): p. 143-155.
11. Myung, D., et al., *Probing the Mechanism of Friction Stir Welding with ALE Based Finite Element Simulations and Its Application to Strength Prediction of Welded Aluminum.* Metals and Materials International, 2021. **27**(4): p. 650-666.
12. Hasan, A.F., C.J. Bennett, and P.H. Shipway, *A numerical comparison of the flow behaviour in Friction Stir Welding (FSW) using unworn and worn tool geometries.* Materials & Design, 2015. **87**: p. 1037-1046.
13. Jedrasiak, P. and H.R. Shercliff, *Small strain finite element modelling of friction stir spot welding*

of Al and Mg alloys. Journal of Materials Processing Technology, 2019. **263**: p. 207-222.
14. He, X., F. Gu, and A. Ball, *A review of numerical analysis of friction stir welding.* Progress in Materials Science, 2014. **65**: p. 1-66.
15. Chen, G., et al., *Thermo-mechanical Analysis of Friction Stir Welding: A Review on Recent Advances.* Acta Metallurgica Sinica (English Letters), 2020. **33**(1): p. 3-12.
16. Salih, O.S., H. Ou, and W. Sun, *Heat generation, plastic deformation and residual stresses in friction stir welding of aluminium alloy.* International Journal of Mechanical Sciences, 2023. **238**: p. 107827.

Nomenclature

Item	Definition
k	Thermal conductivity
$\boldsymbol{\rho}$	Density
Cp	Specific heat capacity
u	Velocity
$\boldsymbol{\mu}$	Friction coefficient
r_p	Pin radius
$\boldsymbol{\omega}$	Pin's angular velocity
$Y(T)$	Average shear stress of the material
F_n	Normal force
A_s	Shoulder's surface area
T_{melt}	Plate's melting temperature
h_u	Heat transfer coefficients for natural convection
h_d	Heat transfer coefficients for natural convection
T_0	Reference temperature
$\boldsymbol{\varepsilon}$	Surface emissivity
$\boldsymbol{\sigma}$	Stefan-Boltzmann constant
T_{amb}	Ambient air temperature